LETTERS

Simulating micrometre-scale crystal growth from solution

Stefano Piana[1], Manijeh Reyhani[1] & Julian D. Gale[1]

Understanding crystal growth is essential for controlling the crystallization used in industrial separation and purification processes. Because solids interact through their surfaces, crystal shape can influence both chemical and physical properties[1]. The thermodynamic morphology can readily be predicted[2], but most particle shapes are actually controlled by the kinetics of the atomic growth processes through which assembly occurs[3]. Here we study the urea–solvent interface at the nanometre scale and report kinetic Monte Carlo simulations of the micrometre-scale three-dimensional growth of urea crystals. These simulations accurately reproduce experimentally observed crystal growth. Unlike previous models of crystal growth[4–6], no assumption is made that the morphology can be constructed from the results for independently growing surfaces or from an *a priori* specification of surface defect concentration. This approach offers insights into the role of the solvent, the degree of supersaturation, and the contribution that extended defects (such as screw dislocations) make to crystal growth. It also connects observations made at the nanometre scale, through *in situ* atomic force microscopy, with those made at the macroscopic level. If extended to include additives, the technique could lead to the computer-aided design of crystals.

The diversity of crystal morphologies that can be found for a single material is testimony to the fact that the macroscopic shape is highly sensitive to the growth conditions, because kinetic control is usually dominant[7]. For example, Fig. 1a and b illustrates two distinct morphologies that are exhibited by the molecular crystalline material urea—$(NH_2)_2CO$—which one is obtained depends on whether the solvent used is water or methanol. There are even variations between individual particles, affected by their age and by when they successfully nucleated relative to other crystallites. The challenge is to be able to predict such behaviour and to reconcile it with atomic detail, such as is becoming available from *in situ* scanning probe microscopy. Here we will demonstrate that computer simulation can provide a means of bridging this gap and make it feasible to explore the crystal growth process with almost no prior assumptions.

It was previously[6] shown that the broad features of the morphology of urea in water could be determined by information obtained from the molecular dynamics simulation of the aqueous interface for both the (001) and (110) surfaces. It was assumed that the system was growing at low supersaturation and therefore that screw dislocations would be the dominant growth site for all faces. Hence, the relative rates of growth are determined on the basis of the thermodynamics of incorporating molecules at kink sites. Now, with the advance of computer power, it is possible[8] to determine the rates directly for all the steps of growth of the urea surface. To achieve this involves classifying the individual urea molecules as being either crystalline or in solution. Crystalline sites are then subdivided according to the local coordination environment of the molecule, based on the number of neighbouring molecules of a given type, as shown in Fig. 2. By literally counting the number of transitions between different sites during several nanoseconds of simulation we can obtain the rate for each step. Note that rates are determined for both the dissolution step, in which a molecule moves from a given crystalline environment to solution, and the crystallization step, which is the reverse process. Examination of the influence of the classification criteria and the sampling methods used indicates that the results are not particularly sensitive to these factors, provided the simulation duration is sufficient.

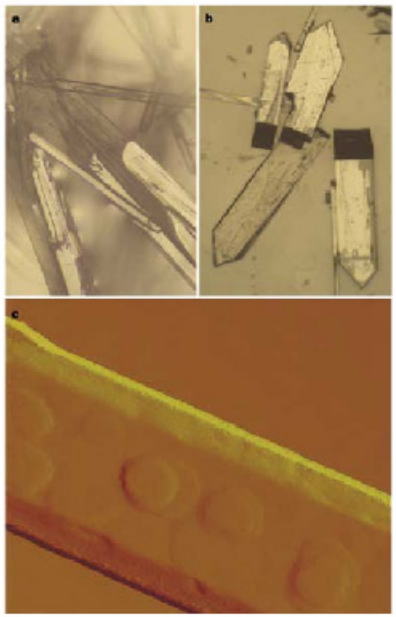

Figure 1 | Optical microscope and scanning probe microscope pictures of urea crystals. **a**, Needle-like morphology characteristic of urea crystals growing from water solution. **b**, Polar morphology of urea crystals growing from a methanol solution. **c**, Scanning probe microscope image of the [110] face of a methanol-grown urea crystal, displaying a morphology typical of a birth-and-spread growth mechanism.

[1]Nanochemistry Research Institute, Department of Applied Chemistry, Curtin University of Technology, GPO Box U1987, Perth 6845, Western Australia

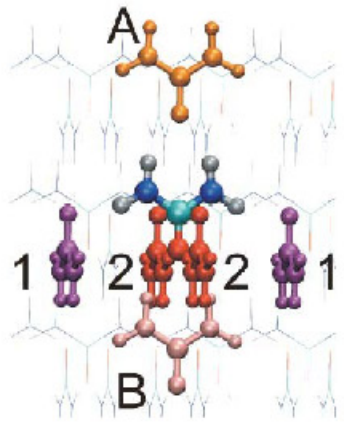

Figure 2 | Characterization of the local environment of a urea molecule. The four symmetry non-equivalent neighbouring molecules to a given urea molecule are illustrated, where the molecules labelled 1 and 2 lie in the same crystallographic **a**–**b** plane, whereas the molecules A and B lie above and below, respectively, along the c axis.

Here we have simulated the solvent–urea interface for both water and methanol, as well as for four different surfaces, namely the (001), (110), (111) and $(-1-1-1)$ cuts. We note that the polar (111) and $(-1-1-1)$ surfaces are non-equivalent. Snapshots from the molecular dynamics trajectories are shown in Fig. 3. In the present methodology, it is not necessary to simulate all possible surfaces to obtain reliable results, as would be the case when determining the thermodynamic morphology according to a Wulff construction[9]. It is sufficient to determine rates for all possible transitions between unique sites that might occur on any surface. In the case of urea, the higher index surfaces can be considered to be faceted versions of the surfaces studied here, so we already have a complete set of surface sites within a nearest-neighbour and next-nearest-neighbour model.

So far, only rates for molecular processes at the nanoscale have been determined because they are extracted from simulations where the system dimensions are of the order of nanometres and the amount of real time sampled is up to 100 ns. However, the smallest observable crystallites in an optical microscope are on the micrometre scale—that is, three orders of magnitude larger—and the timescale for observable growth of a urea crystal is of the order of milliseconds. With current computers it is impractical to simulate crystal growth directly at a macroscopic level. However, by using the rates for individual steps as the probabilities for transitions in a kinetic Monte Carlo[10] simulation it is feasible to make the connection between nanoscale simulation, scanning probe microscopy and the observed morphology of crystals from optical microscopy.

In the kinetic Monte Carlo approach used, each molecule is represented by a point on a grid with the arrangement of the lattice

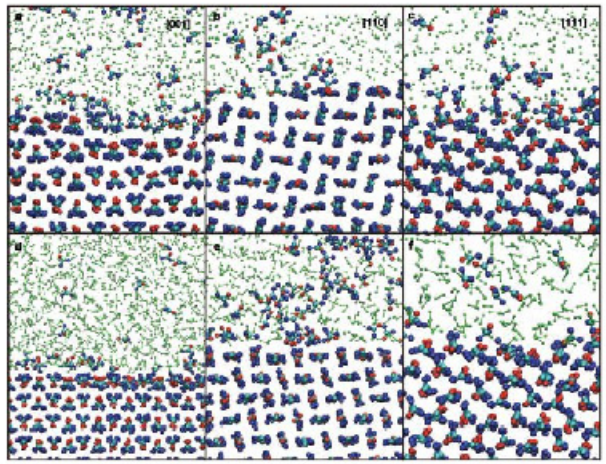

Figure 3 | Snapshots from the molecular dynamics simulations of the urea–solvent interface. **a**–**c**, For water, the frames show the (001) (**a**), (110) (**b**), and (111)–$(-1-1-1)$ (**c**) surfaces. **d**–**f**, As for **a**–**c** but for methanol.

sites of the urea crystal structure. Each site then carries the information of whether it is occupied by a urea molecule, or vacant, and whether the molecular dipole is pointing up or down. The orientation of the dipole is equivalent to defining the plane in which the urea molecule is situated. Sequentially, each site is examined and a pathway is chosen in proportion to the transition probability over a 50-ps interval. Here the time interval is set equal to that used to sample the transitions within the atomistic molecular dynamics. Once all sites have been considered, the clock is advanced by 50 ps and the process repeated. The present method differs from conventional approaches to kinetic Monte Carlo simulations in one important respect: the rates are obtained directly by simulation, whereas normally activation energies are calculated and then rates are estimated based on an approximation of the prefactor[11]. In the context of crystal growth, the present work also deviates from previous studies[12] using kinetic Monte Carlo simulations by considering the full three-dimensional evolution of a crystal, rather than two-dimensional growth of a particular surface.

To initialize the simulations, a growth nucleus is created that is larger than the critical size. The shape can be chosen arbitrarily because during the initial stages the nucleus undergoes dissolution and growth until the stable morphology is achieved. Thereafter crystal growth begins, depending on the degree of supersaturation, C^*, of the urea solution surrounding the nucleus. Here C^* is defined as $([\text{urea}]-[\text{urea}]_s)/[\text{urea}]_s)$, where $[\text{urea}]_s$ is the saturated solution concentration. Interestingly, for small crystal nuclei, ranging in size from 0.12 to 0.01 μm, it was found that $[\text{urea}]_s$ becomes strongly size-dependent and for the small nuclei (~10 nm radius) can be up to 20% higher than the bulk limit.

To control the degree of supersaturation, the fraction of sites that are occupied by a urea molecule in solution can be manipulated. Two sets of conditions can be created—one in which the number of urea molecules is finite, and so C^* decreases with time until growth is halted, and one in which C^* is held constant by replenishing the reservoir of urea molecules as the number is depleted by crystal growth.

Simulations of urea crystals growing from methanol and water solutions at a supersaturation of $C^* = 3 \times 10^{-2}$ were performed. Figure 4a and b shows a comparison of the crystal morphologies obtained from these simulations with the morphology of urea crystals observed with an *in situ* optical microscope. The kinetic Monte Carlo simulation in water indicates that urea crystals grow from aqueous solution as long needles, of aspect ratio greater than 1,000, with large [110] faces and a slightly faceted [001] face. Growth on the [110] faces is not observed at this supersaturation, in agreement with the experimental observation that at a supersaturation of $\sim 10^{-3}$, the growth on the [110] face is more than three orders of magnitude slower than that on the [001] face[13]. In contrast, growth on the [001] face proceeds via a birth-and-spread mechanism where nucleation is not rate-limiting (rough growth).

The morphology emerging from the simulations of growth from a methanol solution is remarkably different from the simulations in water solution. The aspect ratio of methanol-grown crystals is 20–100 times smaller and the [001] faces are unstable, being completely replaced by polar [111] faces (Fig. 4b). All these findings are completely consistent with the optical microscope and scanning probe microscopy images of urea crystals growing from methanol solution (Fig. 1). We find nucleation to be rate-limiting for growth on the [110] face at low to moderate supersaturation ($C^* < 10^{-1}$). This growth mechanism has been confirmed by scanning probe microscopy data (Fig. 1c), in which the surface morphology typical of a birth-and-spread growth mechanism can be clearly identified. We therefore predict the aspect ratio to be size-dependent under these conditions, with values in the range of 10–40.

From the simulations, we can observe exactly why urea exhibits the polar morphology in which the two ends are capped by points twisted by 90 degrees. This is due to the rate of growth of steps on the [110] face from methanol being different in the +c and −c directions (Fig. 4b). On the symmetry-equivalent [110] and [−1 −10] faces, the rate of molecular deposition on steps in the +c direction is twice that in the −c one, while for the [1 −10] and [−110] faces, the situation is reversed. This asymmetry in the growth rate is exhibited by islands growing on the surface, because the initial nucleation site remains close to one edge of the island, rather than being located at the centre.

It has been proposed[9,13] that, at low supersaturation, the presence of screw dislocations is important for the growth of the [001] face. To investigate this issue, we performed two-dimensional kinetic Monte Carlo simulations of a 0.1 × 0.1 μm [001] face, at a supersaturation of 1×10^{-3}, with and without a screw dislocation present. The presence of a screw dislocation is found to accelerate the rate by only 10%. However, on the nucleation-limited [110] face, the introduction of a screw dislocation indeed produces a fivefold enhancement of the growth rate, up to a supersaturation of 3×10^{-2}.

Our results show that it is possible to explore the influence of supersaturation, concentration gradients and diffusion control within the solvent, to name only a few of the many factors that influence crystal growth. Critical nuclei sizes can also readily be determined as a function of conditions. With further atomistic simulations, we may next examine the interplay between impurities, supersaturation and crystal growth[14]. Although it may prove more complex and computationally demanding, this approach is applicable to crystals in general, including species with conformational freedom. Three-dimensional kinetic Monte Carlo simulation, based on rates obtained directly from nanoscale simulation, thus provides a new technique for the predictive design of crystal growth experiments.

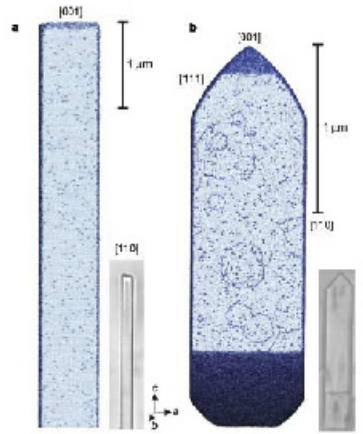

Figure 4 | Comparison of the experimental and theoretical micrometre-scale crystal morphologies. The frames show the results of the kinetic Monte Carlo simulation of a urea crystal growing from solution and the comparable *in situ* optical microscope image for both water (**a**) and methanol (**b**) as the solvent. In the simulated images the shade of a site depends on the local coordination number. Dark, medium and light blue sites are those with three, four and five neighbours, respectively. The birth-and-spread growth patterns observed in the kinetic Monte Carlo simulation of growth from a methanol solution can be compared with the scanning probe microscopy data in Fig. 1c.

METHODS

More details of the methodology are presented in the Supplementary Information.

Atomistic molecular dynamics simulations. Molecular dynamics simulations were performed for the [001], [110] and [111]/[−1−1−1] crystal faces of urea in contact with water (w) and methanol (m) solutions. The initial coordinates were generated with the program GDIS[15] from the unit cell determined by X-ray diffraction[16]. The surface area was 8 × 8, 6 × 6 and 8 × 8 unit cells for the [001], [110] and [111] surfaces, respectively. The depths of the urea slabs were 6, 8 and 5 unit cells, respectively. The two-dimensional cells were converted into three-dimensional cells having the c axis perpendicular to the surface and magnitude 25 Å larger than the unit cell. The gap between the two surfaces was filled with solvent molecules using the genbox[17] program. The final systems consisted of 768, 576 and 320 urea molecules and 1,295, 931 and 631 solvent molecules. All the simulations were run with the program GROMACS[17], using force fields for the urea–urea and urea–solvent interactions previously parameterized[8,18]. The particle mesh Ewald[19] method was used for the long-range electrostatics with a short-range cut-off of 0.9 nm. The time step for the molecular dynamics simulation was 2.0 fs. Further details on the methodology can be found elsewhere[8]. Solvent molecule positions were first relaxed by geometry optimization and then the density of the system was equilibrated by performing 300 ps of molecular dynamics simulation at 300 K with a variable cell along the c axis and the urea molecules fixed. The whole system was equilibrated by performing 200 ps of molecular dynamics simulation at 150 K followed by 800 ps at 300 K. Finally, six simulations of 12, 60 and 12 ns in duration were performed for the [001], [110] and [111]/[−1−1−1] surfaces, respectively, with anisotropic pressure coupling.

Kinetic Monte Carlo simulations. Given the symmetry of the urea crystal, each molecule has four non-equivalent nearest-neighbour sites, illustrated in Fig. 2. When allowing for the possibility of solvent molecules occupying one or more of these positions, this leads to a total of 34 different surface sites types (ten types of kink, eight types of step, four types of terrace sites and 12 types of molecule with one or two urea neighbours only). For many surface sites the second-nearest neighbours have a very limited influence on the reaction rates (less than the statistical error) and so a nearest-neighbour scheme is normally used. However, this is not true for both the step and kink sites, where second-nearest-neighbour information was taken into account in determining reaction rates for these sites.

The calibration of the urea concentration for a saturated solution, $[\text{urea}]_s$, was obtained by performing a kinetic Monte Carlo simulation of a screw dislocation on a two-dimensional periodic 0.6 × 0.6 μm [110] surface at variable concentration. In this simulation a fixed number of molecules are present in the solution and the concentration is depleted as the surface grows around the screw dislocation. The saturated solution concentration was defined as the concentration where the surface neither grows nor dissolves, and was found to be 5 M and for water and 4 M for methanol, respectively. These values can be compared with the experimental values of 11 M (ref. 21) and 4 M (ref. 22), and the previously published[8] saturated solution concentration of 7 M for water, obtained directly by molecular dynamics. The calculated rates are in qualitative agreement with the experiment and appear to capture the larger solubility of urea in water with respect to methanol. Although the simulations underestimate the dissolution of urea in water, this represents an error of only 2 kJ mol^{-1} in the free energy—an amount beyond the accuracy of most theoretical methods at present. Similarly, the discrepancy between the saturated solution concentrations for water in the kinetic Monte Carlo and the explicit simulations represents a very small error in the thermodynamic mapping.

Scanning probe microscopy. Urea crystals were imaged with an atomic force microscope (deflection plot). Crystals were grown from a saturated methanol solution by solvent evaporation and deposited on a mica surface. A Digital Instruments atomic force microscope, operated in contact mode, was used to take images of the crystals.

Received 28 June; accepted 4 August 2005.

1. Winn, D. & Doherty, M. F. Modeling crystal shapes of organic materials grown from solution. *Am. Inst. Chem. Eng. J.* **46**, 1348–1367 (2000).
2. Gibbs, J. W. *Collected Works* (eds Longley, W. R. & van Name, R. G.) (Longman, New York, 1928).
3. Rodriguez-Hornedo, N. & Murphy, D. Significance of controlling crystallization mechanisms and kinetics in pharmaceutical systems. *J. Pharm. Sci.* **88**, 651–660 (1999).
4. Hartman, P. & Perdok, W. G. On the relations between structure and morphology of crystals. *Acta Crystallogr.* **8**, 48–52 (1955).
5. Pina, C. M., Becker, U., Risthaus, P., Bosbach, D. & Putnis, A. Molecular-scale mechanisms of crystal growth of barite. *Nature* **395**, 483–486 (1998).
6. Liu, X. Y., Boek, E. S., Briels, W. J. & Bennema, P. Prediction of crystal growth morphology based on structural analysis of the solid-fluid interface. *Nature* **374**, 342–345 (1995).
7. Davey, R. J., Mullin, J. W. & Whiting, M. J. L. Habit modification of succinic acid crystals grown from different solvents. *J. Cryst. Growth* **58**, 304–312 (1982).
8. Piana, S. & Gale, J. D. Understanding the barriers to crystal growth: Dynamical simulation of the dissolution and growth of urea from aqueous solution. *J. Am. Chem. Soc.* **127**, 1975–1982 (2005).
9. Wulff, G. Zur frage der geschwindigkeith des wachsthums und der auflosung der krystallflachen. *Z. Krist.* **34**, 449–530 (1901).
10. Gillespie, D. T. A general method for numerically simulating the stochastic time evolution of coupled chemical reactions. *J. Comp. Phys.* **22**, 403–434 (1976).
11. Jónsson, H. Theoretical studies of atomic scale processes relevant to crystal growth. *Annu. Rev. Phys. Chem.* **51**, 623–653 (2000).
12. Boerrigter, S. X. M. *et al.* MONTY: Monte Carlo crystal growth on any crystal structure in any crystallographic orientation; application to fats. *J. Phys. Chem. A* **108**, 5894–5902 (2004).
13. Davey, R., Fila, W. & Garside, J. The influence of biuret on the growth kinetics of urea crystals from aqueous solutions. *J. Cryst. Growth* **79**, 607–613 (1986).
14. Land, T. A., Martin, T. L., Potapenko, S., Palmore, G. T. & de Yoreo, J. J. Recovery of surfaces from impurity poisoning during crystal growth. *Nature* **399**, 442–445 (1999).
15. Fleming, S. D. & Rohl, A. L. GDIS: a visualization program for molecular and periodic systems. *Z Krist.* **220**, 1–5 (2005).
16. Swaminathan, S., Craven, B. M., Spackman, M. A. & Stewart, R. F. Theoretical and experimental studies of the charge density in urea. *Acta Crystallogr. B* **40**, 398–404 (1984).
17. Lindhal, E., Hess, B. & van der Spoel, D. GROMACS 3.0: a package for molecular simulation and trajectory analysis. *J. Mol. Modeling* **7**, 306–317 (2001).
18. Smith, L. J., Berendsen, H. J. C. & van Gusteren, W. F. Computer simulation of urea-water mixtures: A test of force field parameters for use in biomolecular simulation. *J. Phys. Chem. B* **108**, 1065–1071 (2004).
19. van Gusteren, W. F., *et al. Biomolecular Simulation: the GROMOS96 Manual and User Guide* 1–1024 (Vdf Hochschulverlag AG an der ETH Zurich, Zurich, 1996).
20. Essman, U. *et al.* A smooth particle mesh Ewald method. *J. Chem. Phys.* **103**, 8577–8593 (1995).
21. Pinck, L. A. & Kelly, M. A. The solubility of urea in water. *J. Am. Chem. Soc.* **47**, 2170–2172 (1925).
22. Boomadevi, S., Dhanesekaran, R. & Ramasamy, P. Investigations on nucleation and growth kinetics of urea crystals from methanol. *Cryst. Res. Technol.* **37**, 159–168 (2002).

Supplementary Information is linked to the online version of the paper at www.nature.com/nature.

Acknowledgements We are grateful to A. Rohl for discussions, and to T. Dincer for assistance with the optical microscope. S.P. acknowledges financial support from an Australian Research Fellowship, while S.P. and J.D.G. both gratefully acknowledge the support of the Government of Western Australia through the Premiers Research Fellowship programme.

Author Contributions S.P. performed all the calculations and the optical microscopy, M.R. produced the atomic force microscope images, J.D.G. conceived the project and wrote the manuscript with S.P.

Author Information Reprints and permissions information is available at npg.nature.com/reprintsandpermissions. The authors declare no competing financial interests. Correspondence and requests for materials should be addressed to J.D.G. (J.Gale@curtin.edu.au).